



Low-Threshold Bidirectional Air Lasing

Alexandre Laurain, Maik Scheller, and Pavel Polynkin*

College of Optical Sciences, University of Arizona, 1630 East University Boulevard, Tucson, Arizona 85721, USA

(Received 23 August 2014; published 17 December 2014)

Air lasing refers to the remote optical pumping of the constituents of ambient air that results in a directional laserlike emission from the pumped region. Intense current investigations of this concept are motivated by the potential applications in remote atmospheric sensing. Different approaches to air lasing are being investigated, but, so far, only the approach based on dissociation and resonant two-photon pumping of air molecules by deep-UV laser pulses has produced measurable lasing energies in real air and in the backward direction, which is of the most relevance for applications. However, the emission had a high pumping threshold, in hundreds of GW/cm^2 . We demonstrate that the threshold can be virtually eliminated through predissociation of air molecules with an additional nanosecond laser. We use a single tunable pump laser system to generate backward-propagating lasing in both oxygen and nitrogen in air, with energies of up to $1 \mu\text{J}$ per pulse.

DOI: [10.1103/PhysRevLett.113.253901](https://doi.org/10.1103/PhysRevLett.113.253901)

PACS numbers: 42.55.Lt, 33.80.Gj, 33.80.Rv, 42.68.Ca

The development of a viable approach to the generation of remote, optically pumped, directional light source in ambient air could revolutionize the field of remote atmospheric sensing [1]. Air lasers emitting backwards, i.e., from a remote location in the sky towards the observer on the ground, would be of the most practical utility. The application of such remote backward-propagating optical probes will result in dramatically higher detection signals compared to those attainable through the use of weak backscattering of forward-propagating laser beams. Remote sensing schemes using yet-to-be-developed efficient backward-emitting air lasers have been recently discussed [2,3].

Nature offers limited options for the gain medium of an air laser. Only oxygen and nitrogen are present in significant amounts in the atmosphere. Thus molecular, atomic, or ionic forms of these two gases will have to be used. Another practical constraint is associated with the traveling-wave pumping configuration intrinsic to air lasing. Such an excitation geometry typically favors the generation of forward-propagating over backward-propagating emission. Notwithstanding these obstacles, several approaches to air lasing have been the subjects of intense ongoing investigations. One approach is based on femtosecond laser filamentation [4–7]. Impulsive lasing in this case is either very weak, and detectable only with photomultipliers, or forward propagating. Pumping with mid-IR femtosecond pulses has been shown to produce radiation in the backward direction, but so far only in a nitrogen-argon mixture [8]. Another approach is based on optically driven electron impact excitation of neutral nitrogen molecules in air resulting in gain at a 337-nm wavelength [9]. So far, that approach has resulted in the generation of emission in the forward direction only [10]. Nonlinear wavelength conversion in air has also been

discussed as a potential source of air lasing. Because of phase-matching constraints, that approach also favors emission in the forward direction [11].

At the time of this writing, the only approach that succeeded in the generation of backward-propagating lasing with quantifiable pulse energies in the atmospheric air was based on the excitation of air molecules by laser pulses at specific deep-UV wavelengths. Pumping atmospheric oxygen with laser pulses at a 226-nm wavelength resulted in backward emission at 845 nm [12,13] while pumping atmospheric nitrogen at 207 nm yielded backward lasing at around 745 nm [14]. Rather complex pump laser systems were used in those demonstrations. In the case of oxygen emission, either the second harmonic of a sum-frequency signal of a titanium:sapphire and Nd:YAG lasers [12] or a sum-frequency signal of a third harmonic of a Nd:YAG laser and a dye laser, operating at a 622-nm wavelength [13] was used. In the case of nitrogen emission, the pumping was by the fourth harmonic of an ultrafast titanium:sapphire regenerative amplifier [14]. More importantly, backward lasing in those demonstrations had a high threshold, in hundreds of GW/cm^2 , which is an important limitation for the implementation of this approach at a standoff range.

In the above demonstrations, deep-UV pumping served two purposes: First, it dissociated air molecules. Then it excited, through two-photon-resonant pumping, the resulting neutral oxygen or nitrogen atoms. The relevant atomic energy-level diagrams for the cases of excitation of oxygen and nitrogen atoms are shown in Figs. 1(a) and 1(b). The second excitation step, which is the two-photon-resonant pumping of oxygen or nitrogen atoms, necessitates the use of specific deep-UV pump wavelengths, but the dissociation step does not. In this Letter we show that by predissociating oxygen and nitrogen molecules by an

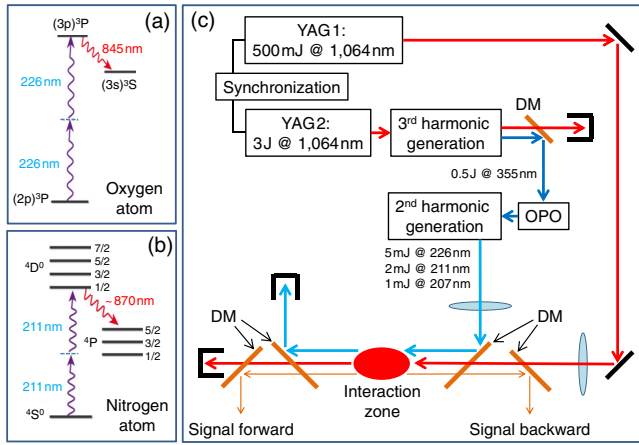


FIG. 1 (color online). (a) Energy level diagram for atomic oxygen showing relevant transitions for resonant two-photon pumping at a 226-nm wavelength and emission at 845 nm. (b) Same for atomic nitrogen. Two-photon pumping is resonant at a wavelength of around 211 nm and emission occurs on various lines at around 870 nm. Another option for pumping nitrogen exists, with resonant two-photon transition to the $4S^0$ level instead of $4D^0$. In that case, two-photon pumping is resonant at a 207-nm wavelength and the lasing occurs at 745 nm [14]. (c) Schematic of the experimental setup. DM: Dichroic Mirror.

auxiliary nanosecond Nd:YAG laser, emission thresholds with respect to the intensity of the tunable deep-UV pump radiation can be virtually eliminated. We further show that backward-propagating lasing with energy of up to $1 \mu\text{J}$ per pulse can be achieved on various transitions of oxygen and nitrogen in air using a single compact, all-solid-state, tunable laser system.

Our experimental setup is schematically shown in Fig. 1(c). Oxygen and nitrogen molecules in ambient air are dissociated by a dedicated Nd:YAG laser generating 500 mJ of energy per pulse at a wavelength of $1.064 \mu\text{m}$. The resulting neutral oxygen and nitrogen atoms are excited by a wavelength-tunable optical parametric oscillator (OPO) system frequency doubled into deep UV. The optical beams produced by the predissociating laser and by the deep-UV OPO are focused by lenses with focal lengths of 20 cm and 10 cm, respectively, and spatially combined using a dichroic mirror. Both light sources produce 6-ns-long pulses at the pulse repetition rate of 10 Hz. The pulse trains from the two systems are temporally synchronized through a common electronic triggering. The deep-UV pulse lags the predissociating pulse in time by several microseconds. Lasing signals produced in the interaction zone in the backward and forward directions are separated from the pump light using dichroic mirrors, filtered by dispersive prisms and analyzed by a spectrometer, energy meter, and fast photodiodes.

We first discuss experimental results obtained with the predissociating laser turned off. This is the same situation as the one discussed in the recent publications on air lasing

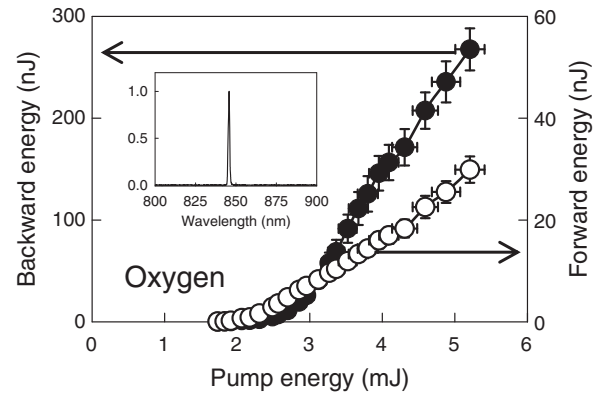


FIG. 2. Energy output of the backward and forward air lasing, vs energy of the deep-UV pump pulse, for the case of atmospheric oxygen. The predissociating Nd:YAG laser is turned off. The pump is tuned to a 226-nm wavelength. The spectrum of backward air lasing is shown in the inset.

[12–14] and in earlier works on two-photon spectroscopy of oxygen and nitrogen atoms in flames [15,16]. Note that similar two-photon-excited stimulated emissions have been investigated in other gases including hydrogen [17], krypton and xenon [18,19], and carbon monoxide [20,21].

The plots for the energy of stimulated emission in the backward and forward directions, for the cases of the pump wavelength tuned to 226 nm and 211 nm, are shown in Figs. 2 and 3, respectively. In the case of 226-nm pumping, the emission results from dissociation and excitation of atmospheric oxygen, while with 211-nm pumping, the emission is due to the dissociation and pumping of nitrogen. Backward-emitted energies are in the range of hundreds of nanojoules and hundreds of picojoules for the cases of oxygen and nitrogen emissions, respectively. In both cases, emissions have high thresholds, in hundreds of GW/cm^2 . In what follows, we will show that those lasing thresholds are in fact thresholds for dissociation of oxygen and nitrogen molecules. Also, in both the oxygen and

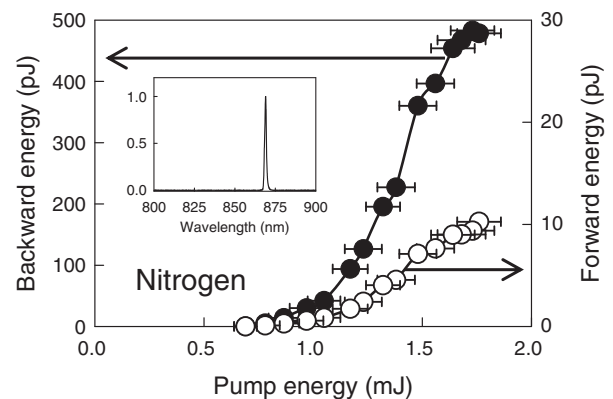


FIG. 3. Same as Fig. 2, but for the case of atmospheric nitrogen. The pump wavelength in this case is tuned to 211 nm. The predissociating nanosecond laser is turned off.

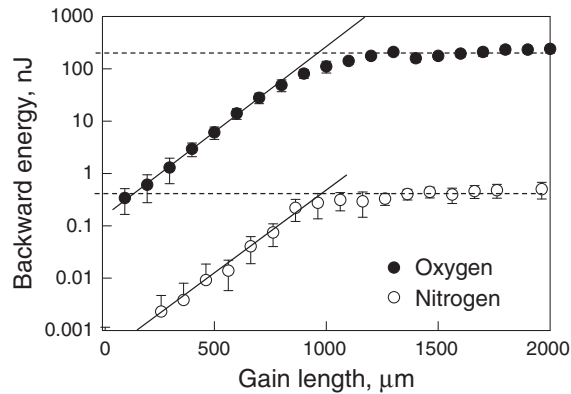


FIG. 4. Log-scale plot of the energy of the backward-lasing signal as a function of the length of the gain region. Gain length is defined by the insertion of a tilted glass plate into the beam path, as described in the text. The two curves are for the cases of 226-nm pumping (oxygen lasing) and 211-nm pumping (nitrogen lasing). Fitting the exponential parts of the gain curves yields gain constants of 74 cm^{-1} and 71 cm^{-1} , for the oxygen and nitrogen cases, respectively.

nitrogen cases, the transient emissions in the backward direction are significantly more energetic than those in the forward direction. (We have also obtained lasing from nitrogen pumped at a 207-nm wavelength. In that case, maximum backward-emitted energy at 745 nm was about 60 pJ.)

By inserting a glass plate into the interaction zone and measuring the backward-propagating signal as a function of the position of the plate, we were able to quantify the energy gain experienced by the backward-propagating lasing signal as it traveled through the amplifying medium. The terminating glass plate was significantly tilted to eliminate any possibility of seeding of the backward emission by the forward-propagating lasing reflected from the plate's surface. The data for gain measurements, which were performed with the predissociating laser turned off, are shown in Fig. 4. The total gain length, for both the oxygen- and nitrogen-lasing cases, is about 1 mm. For oxygen, the gain is exponential for the first ~ 0.75 -mm-long part of the gain medium, yet most of the energy accumulation occurs within the last ~ 250 - μm -long part, where the gain is saturated by the signal. For nitrogen, the gain is exponential through essentially the entire length of the active region. The measured exponential gain constants are 74 cm^{-1} and 71 cm^{-1} , for the cases of oxygen and nitrogen (pumped at a 211-nm wavelength), respectively. These gain values are consistent with the value reported in [12].

The identification of the physical mechanism responsible for air lasing in the forward and backward directions is not trivial. Emission schemes essentially identical to the one used here were extensively studied from 1970s to early 1990s in alkali metal vapors [22–30]. It was established that four emission mechanisms can be operative: The population-inversion-based gain (or amplified spontaneous

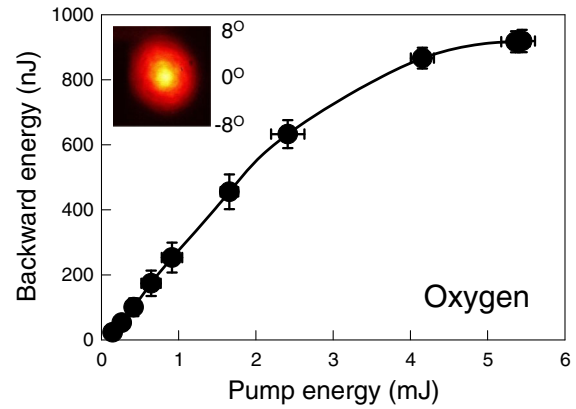


FIG. 5 (color online). Energy output of backward-propagating air lasing, vs energy of the deep-UV pump pulse, for the case of atmospheric oxygen emission and with the predissociating Nd:YAG laser turned on. The wavelength of the tunable OPO pump is set to 226 nm. The threshold with respect to the energy of the deep-UV pump is essentially absent. The inset shows the far-field intensity profile of the generated backward-propagating laser beam with the angular FWHM beam divergence of about 6° .

emission) which is about equally effective in both forward and backward directions, the hyper-Raman gain, which is also about equally effective in both directions, four-wave mixing, which produces emission only in the forward direction, and, finally, exotic emission mechanisms such as superfluorescence and superradiance [13,31]. Different gain mechanisms can dominate in different parts of the gain zone under different conditions. It was also shown that under rather general conditions the hyper-Raman gain and four-wave mixing interfere destructively in the forward direction, resulting in the predominant emission backwards [27–30].

We now discuss the results obtained with the predissociating nanosecond laser turned on. The corresponding energy curves for the cases of oxygen and nitrogen emissions are shown in Figs. 5 and 6, respectively. The corresponding beam intensity profiles for the backward emission are shown in the insets. In both cases shown, the FWHM beam divergence is about 6° , which is consistent with the 10 - μm diameter of the focused pump beam in the interaction zone. Remarkably, emission thresholds with respect to the deep-UV pump energy are essentially absent. We were unable to reliably quantify the thresholds in these cases because they were below our measurement uncertainty. The laser energy initially shows a linear growth with respect to the pump energy, followed by a roll-off. The linear slope of the energy curves suggests that for both the oxygen- and nitrogen-lasing cases, the gain media are saturated by the lasing signal starting from very low levels of pumping. The maximum energy obtained in the backward direction for the case of oxygen emission is about $1 \mu\text{J}$. The maximum energy obtained from nitrogen lasing with 211-nm pumping is about 100 nJ, which is more than

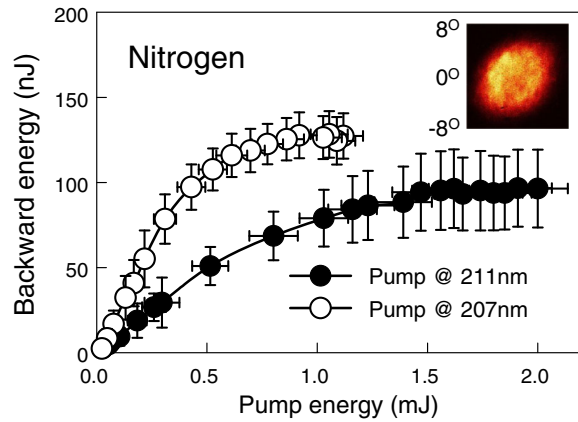


FIG. 6 (color online). Same as Fig. 5 but for the case of atmospheric nitrogen pumped at 211-nm or 207-nm wavelengths. The inset shows the far-field intensity profile of the generated backward-propagating laser beam.

2 orders of magnitude higher than that in the case without predissociation.

In the data shown, the energy of the predissociating laser pulse at a 1064-nm wavelength is 500 mJ. The effect has a thresholdlike dependence on the energy of the predissociating pulse, with the value of threshold approximately coinciding with that for the appearance of an optical breakdown of laboratory air (about 100 mJ under our focusing conditions). The backward-lasing energy is fairly insensitive to the exact value of the delay between the predissociating and deep-UV pump pulses, when the delay is in the range between 500 ns and several microseconds. These observations suggest that the dissociation of nitrogen and oxygen molecules is driven by electron impact within the optical breakdown region produced by the predissociating laser pulse. The temporal delay between the predissociating and pump pulses is necessary for the defocusing effects from free electrons and from the pressure reduction on the beam axis to dissipate.

The maximum range at which the air lasing approach discussed here can be implemented will be ultimately limited by air absorption of the deep-UV pump beam. Based on the measurements of absorption cross sections for deep-UV light in the atmosphere [32], the range at which linear absorption of air results in a 50% reduction of the deep-UV pump light is about 250 m and 130 m, for pump wavelengths of 226 nm and 211 nm, respectively. Thus the maximum range limited by air absorption can be estimated at a few hundred meters. At this kind of range air turbulence should be manageable through the use of adaptive optics.

The polarization of both forward- and backward-propagating air lasing in the case of oxygen is always linear and parallel to the direction of the linear polarization of the deep-UV pumping laser beam. That suggests a coherent impulsive nature of excitation. For the case of nitrogen, the degree of polarization of the generated lasing depends on the particular transition being pumped within

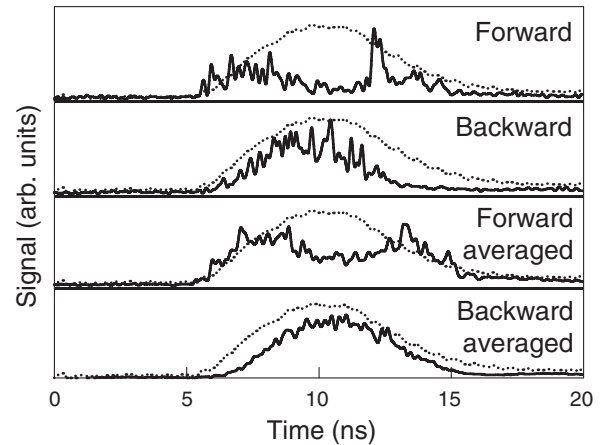


FIG. 7. Temporal waveforms of the forward and backward oxygen lasing with predissociation. In all plots, the solid lines show lasing waveforms and the dotted lines show the temporal waveform of the deep-UV pump pulse. Two bottom panels show temporal emission waveforms averaged over ten laser shots. The averaged forward and backward signals are out of phase, evidencing gain competition between the two signals.

the fine structure of the upper lasing level. This variability is caused by a complex fine structure of the spectrum of atomic nitrogen.

Finally, temporal waveforms of the forward and backward emissions were recorded with two identical 5-GHz InGaAs photodetectors and a digital oscilloscope with 6-GHz bandwidth. The recorded waveforms show spiky structures, similar to those reported in [13,31]. We were unable to confirm a correlation between the timing of the spikes in the forward- and backward-propagating signals with each other or with the modulation of the temporal intensity envelope of the pumping laser pulse. However, when emission waveforms are averaged over several shots, as in the example shown in Fig. 7, a pattern emerges that indicates that the forward- and backward-propagating waves, on average, compete for optical gain.

In conclusion, we have reported experiments on air lasing under resonant two-photon pumping by tunable deep-UV laser pulses. Backward and forward emissions on various lines of oxygen and nitrogen are generated under pumping by a single compact, all-solid-state, tunable laser system. Predissociation of oxygen and nitrogen molecules in the air by an additional Nd:YAG laser results in a virtual elimination of the lasing threshold with respect to the intensity of the deep-UV pump radiation. Backward-propagating emission with the energy per pulse of up to 1 μ J is demonstrated. The range limitation for the approach discussed here can be estimated at a few hundred meters.

The authors acknowledge helpful discussions with Victor Hasson and Jerome Moloney. This work was supported by the United States Air Force Office of

Scientific Research under Programs No. FA9550-12-1-0143, No. FA9550-12-1-0482, and No. FA9550-10-1-0561, and by the Defense Threat Reduction Agency (DTRA) under Program No. HDTRA 1-14-1-0009.

*ppolynkin@optics.arizona.edu

- [1] P. R. Hemmer, R. B. Miles, P. Polynkin, T. Siebert, A. V. Sokolov, P. Sprangle, and M. O. Scully, *Proc. Natl. Acad. Sci. U.S.A.* **108**, 3130 (2011).
- [2] L. Yuan, A. A. Lanin, P. K. Jha, A. J. Traverso, D. V. Voronine, K. E. Dorfman, A. B. Fedotov, G. R. Welch, A. V. Sokolov, A. M. Zheltikov, and M. O. Scully, *Laser Phys. Lett.* **8**, 736 (2011).
- [3] P. N. Malevich, D. Kartashov, Z. Pu, S. Alisauskas, A. Pugzlys, A. Baltuska, L. Giniunas, R. Danielius, A. A. Lanin, A. M. Zheltikov, M. Marangoni, and G. Cerullo, *Opt. Express* **20**, 18784 (2012).
- [4] Q. Luo, W. Liu, and S. L. Chin, *Appl. Phys. B* **76**, 337 (2003).
- [5] J. Yao, B. Zeng, H. Xu, G. Li, W. Chu, J. Ni, H. Zhang, S. L. Chin, Y. Cheng, and Z. Xu, *Phys. Rev. A* **84**, 051802(R) (2011).
- [6] Y. Liu, Y. Brelet, G. Point, A. Houard, and A. Mysyrowicz, *Opt. Express* **21**, 22791 (2013).
- [7] T.-J. Wang, J. Ju, J.-F. Daigle, S. Yuan, R. Li, and S. L. Chin, *Laser Phys. Lett.* **10**, 125401 (2013).
- [8] D. Kartashov, S. Alisauskas, G. Andriukaitis, A. Pugzlys, M. Shneider, A. Zheltikov, S. L. Chin, and A. Baltuska, *Phys. Rev. A* **86**, 033831 (2012).
- [9] P. Sprangle, J. Penano, B. Hafizi, D. Gordon, and M. Scully, *Appl. Phys. Lett.* **98**, 211102 (2011).
- [10] D. Kartashov, S. Alisauskas, A. Baltuska, A. Schmitt-Sody, P. Roach, and P. Polynkin, *Phys. Rev. A* **88**, 041805(R) (2013).
- [11] M. Scheller, X. Chen, G. O. Ariunbold, N. Born, J. Moloney, M. Kolesik, and P. Polynkin, *Phys. Rev. A* **89**, 053805 (2014).
- [12] A. Dogariu, J. B. Michael, M. O. Scully, and R. B. Miles, *Science* **331**, 442 (2011).
- [13] A. J. Traverso, R. Sanchez-Gonzalez, L. Yuan, K. Wang, D. V. Voronine, A. M. Zheltikov, Y. Rostovtsev, V. A. Sautenkov, A. V. Sokolov, S. W. North, and M. O. Scully, *Proc. Natl. Acad. Sci. U.S.A.* **109**, 15185 (2012).
- [14] A. Dogariu and R. B. Miles, in *Frontiers in Optics 2013/ Laser Science XXIX, Orlando, Florida, 2013* (Laser Science, Orlando, 2013).
- [15] M. Alden and U. Westblom, *Opt. Lett.* **14**, 305 (1989).
- [16] S. Agrup and M. Alden, *Chem. Phys. Lett.* **170**, 406 (1990).
- [17] J. E. M. Goldsmith, *J. Opt. Soc. Am. B* **6**, 1979 (1989).
- [18] M. B. Rankin, J. P. Davis, C. Giranda, and L. C. Bobb, *Opt. Commun.* **70**, 345 (1989).
- [19] J. C. Miller, *Phys. Rev. A* **40**, 6969 (1989).
- [20] U. Westblom, S. Agrup, M. Alden, H. M. Hertz, and J. E. M. Goldsmith, *Appl. Phys. B* **50**, 487 (1990).
- [21] H. Bergstrom, H. Lunberg, and A. Persson, *Z. Phys. D* **21**, 323 (1991).
- [22] F. A. Korolev, S. A. Bakhranov, and V. I. Odintsov, *Pis'ma v ZhETF* **12**, 131 (1970) [*JETP Lett.* **12**, 90 (1970)].
- [23] Q. H. F. Vreken and H. M. J. Hiksloops, *Opt. Commun.* **21**, 127 (1977).
- [24] D. Cotter, D. C. Hanna, W. H. W. Tuttlebee, and M. A. Yuratich, *Opt. Commun.* **22**, 190 (1977).
- [25] J. Reif and H. Walther, *Appl. Phys.* **15**, 361 (1978).
- [26] D. Krokkel, K. Ludewigt, and H. Welling, *IEEE J. Quantum Electron.* **22**, 489 (1986).
- [27] R. W. Boyd, M. S. Malcuit, D. J. Gauthier, and K. Rzazewski, *Phys. Rev. A* **35**, 1648 (1987).
- [28] M. A. Moore, W. R. Garrett, and M. G. Payne, *Opt. Commun.* **68**, 310 (1988).
- [29] Yu. P. Malakyan, *Opt. Commun.* **69**, 315 (1989).
- [30] W. R. Garrett, M. A. Moore, R. C. Hart, M. G. Payne, and R. Wunderlich, *Phys. Rev. A* **45**, 6687 (1992).
- [31] L. Yuan, B. H. Hokr, A. J. Traverso, D. V. Voronine, Y. Rostovtsev, A. V. Sokolov, and M. O. Scully, *Phys. Rev. A* **87**, 023826 (2013).
- [32] V. Hasson and R. W. Nichols, *J. Phys. B* **4**, 1789 (1971).